Perennial snow and ice variations (2000–2008) in the Arctic circumpolar land area from satellite observations

F. M. A. Fontana,[1,2] A. P. Trishchenko,[3,4] Y. Luo,[3,4] K. V. Khlopenkov,[3,5] S. U. Nussbaumer,[1] and S. Wunderle[1]

Received 17 January 2010; revised 29 July 2010; accepted 5 August 2010; published 11 November 2010.

[1] Perennial snow and ice (PSI) extent is an important parameter of mountain environments with regard to its involvement in the hydrological cycle and the surface energy budget. We investigated interannual variations of PSI in nine mountain regions of interest (ROI) between 2000 and 2008. For that purpose, a novel MODIS data set processed at the Canada Centre for Remote Sensing at 250 m spatial resolution was utilized. The extent of PSI exhibited significant interannual variations, with coefficients of variation ranging from 5% to 81% depending on the ROI. A strong negative relationship was found between PSI and positive degree-days (threshold 0°C) during the summer months in most ROIs, with linear correlation coefficients (r) being as low as r = −0.90. In the European Alps and Scandinavia, PSI extent was significantly correlated with annual net glacier mass balances, with r = 0.91 and r = 0.85, respectively, suggesting that MODIS-derived PSI extent may be used as an indicator of net glacier mass balances. Validation of PSI extent in two land surface classifications for the years 2000 and 2005, GLC-2000 and Globcover, revealed significant discrepancies of up to 129% for both classifications. With regard to the importance of such classifications for land surface parameterizations in climate and land surface process models, this is a potential source of error to be investigated in future studies. The results presented here provide an interesting insight into variations of PSI in several ROIs and are instrumental for our understanding of sensitive mountain regions in the context of global climate change assessment.

Citation: Fontana, F. M. A., A. P. Trishchenko, Y. Luo, K. V. Khlopenkov, S. U. Nussbaumer, and S. Wunderle (2010), Perennial snow and ice variations (2000–2008) in the Arctic circumpolar land area from satellite observations, *J. Geophys. Res.*, *115*, F04020, doi:10.1029/2010JF001664.

1. Overview

[2] Snow and ice are important components of the hydrological cycle in many mountain ecosystems [*Beniston*, 2003]. As natural stores of frozen water, they are strongly involved in the modification of the timing and magnitude of water discharge from mountain areas on various temporal scales [*Jansson et al.*, 2003]. Snow and ice are thereby important modulators of water availability both in mountain regions as well as in surrounding lowlands and provide water supply for a significant part of the Earth's population [*Barnett et al.*, 2005]. Furthermore, hydroelectric power plants as sources of renewable energy heavily rely on water temporarily stored in these reservoirs [*Hauenstein*, 2005]. Apart from issues directly related to water resources, snow and ice exert large influences on climate and the surface energy budget on various spatial scales through their typically high albedo or the cooling of the atmosphere [e.g., *Groisman et al.*, 1994; *Vavrus*, 2007]. As a result, they are critical components to be considered for the assessment of land surface–atmosphere interactions [*Nolin and Frei*, 2001; *Kotlarski*, 2007]. On the other hand, variations of snow and ice cover provide some of the clearest evidence of climate change since both snow and ice are often close to the melting point, and therefore react sensitively to changes in temperature [*United Nations Environment Programme*, 2007].

[3] In view of this importance of snow and ice cover for mountain environments from a wide range of aspects, the study of past, present, and future snow and ice cover variations has become increasingly important within the global climate change discussion [*Lemke et al.*, 2007]. In this

[1]Oeschger Centre for Climate Change Research and Institute of Geography, University of Bern, Bern, Switzerland.
[2]Presently at Integrated Remote Sensing Studio, Department of Forest Resources Management, University of British Columbia, Vancouver, British Columbia, Canada.
[3]Canada Centre for Remote Sensing, Ottawa, Ontario, Canada.
[4]Environment Canada, Ottawa, Ontario, Canada.
[5]Science Systems and Applications, Inc., Hampton, Virginia, USA.

0148-0227/10/2010JF001664

context, variation in the spatial extent of perennial snow and ice (PSI) is a key aspect. Perennial snow and ice extent represents minimum snow and ice conditions in mountain regions for a specific year, which are typically observed at the end of the summer season. While interannual changes in the spatial extent of perennial mountain ice, i.e., glaciers and ice caps, are generally small and lag behind climatic changes by at least a few years [*Oerlemans*, 2001], larger year-to-year variability is expected for perennial snow cover due to the close relationship of snow cover with meteorological conditions such as the amount of precipitation and air temperature variations [*Robinson and Dewey*, 1990; *Brown and Mote*, 2009].

[4] Satellite remote sensing provides the unique opportunity to study PSI at a wide range of spatial and temporal scales. For studies of perennial mountain ice, data from high spatial resolution (≤30 m) sensors are the premier source of information [*Kargel et al.*, 2005; *Paul et al.*, 2007], even though the observation frequency of these sensor systems is limited as a consequence of the generally low ground repeat cycles combined with the influence of cloud cover. Studies on snow cover mainly utilized the daily and weekly satellite maps of the Northern Hemisphere snow cover at a spatial resolution of several kilometers [*Robinson et al.*, 1993; *Ramsay*, 1998; *Romanov et al.*, 2002], however, their use for studies of mountain regions is limited because of the relatively coarse spatial resolution. Improved snow cover products have become available with the advent of the Moderate Resolution Imaging Spectroradiometer (MODIS) onboard the Terra and Aqua satellites [*Salomonson et al.*, 1989; *Justice et al.*, 1998], which offers improved snow and ice detection capabilities due to better spectral coverage and finer spatial resolution. The MODIS snow and ice products are available at a range of temporal (daily to monthly) and spatial resolutions (500 m to 0.05°) as described by *Hall et al.* [2002]. However, higher spatial resolution is desirable for studies in rugged terrain in order to capture the patchy appearance of snow cover [*Sirguey et al.*, 2009]. In addition, the Global Climate Observing System (GCOS) has recommended a spatial resolution of 250 m for many Essential Climate Variables (ECVs) intended for terrestrial applications, such as snow cover and albedo [*Global Climate Observing System*, 2006, Appendix 2]. To meet these requirements and as a contribution to the Canadian component of the International Polar Year (IPY) Programme, a MODIS data set at 250 m spatial resolution in all seven land bands (MODIS spectral bands B1–B7) was recently produced by the Canada Centre for Remote Sensing (CCRS) [*Trishchenko et al.*, 2009]. The data set covers the Arctic circumpolar area (ACA; 9000 × 9000 km^2) and is centered at the geographic North Pole.

[5] Not only does this data set represent a valuable tool for the quantification of variations in PSI extent at fine spatial resolution, but it also bears high potential for the validation of land surface classifications (LSCs) in various geographical conditions including complex and spatially heterogeneous mountain regions. Latter application is of particular interest, since LSCs, which are often generated based on remote sensing data, are commonly employed to derive land surface parameter data sets for the use in climate and land surface process models [*Sellers et al.*, 1996; *Bonan et al.*, 2002; *Hagemann*, 2002]. Given the importance of snow and ice for the water and energy budget as outlined above, accurate delineation of permanently snow and ice covered surfaces in such classifications is required. The problem with LSCs is, however, that they differ with regard to the classification schemes employed, underlying remote sensing data, and the time period considered. As a result, classifications may differ considerably [*Hansen and Reed*, 2000; *Giri et al.*, 2005], which emphasizes the motivation to validate PSI extent in LSCs using the newly available MODIS data set produced at the CCRS.

[6] The paper is structured as follows: the CCRS MODIS data set as well as the two freely available global LSCs used in this study, the Global Land Cover 2000 database (GLC-2000) and the Globcover land cover map in 2005, are introduced in section 2. Interannual PSI variations in a number of mountain regions within the ACA are quantified and discussed in section 3.1. Section 3.2 makes use of MODIS-retrieved PSI extent to validate the extent of surfaces classified as PSI in both LSCs as mentioned above. Results are summarized in section 4.

2. Data and Methods

2.1. MODIS Data

[7] The MODIS clear-sky composites for the ACA were generated as described in detail by *Trishchenko et al.* [2009]. In summary, processing includes four major steps: since only bands B1 and B2 of the MODIS sensor are available at 250 m spatial resolution, bands B3 to B7 are downscaled from 500 m to 250 m spatial resolution using an adaptive regression and normalization scheme in a first step [*Trishchenko et al.*, 2006]. Second, bands B1 to B7 are reprojected from swath to Lambert Azimuthal Equal Area (LAEA) projection using a gradient search method [*Khlopenkov and Trishchenko*, 2008], which was shown to preserve the geolocation accuracy achieved by the MODIS science team [*Wolfe et al.*, 2002]. In a third step, scene identification at 250 m resolution is performed using bands B1, B2, B3, and B6. This latter step outputs a mask delineating cloud cover, cloud shadows, and areas observed under clear-sky conditions including information on snow cover. This mask is used in step four together with a set of decision rules to create clear-sky composites for a predefined time interval [*Luo et al.*, 2008]. Data from MODIS on the Terra spacecraft were used because of band-to-band registration issues for MODIS on the Aqua spacecraft [*Xiong et al.*, 2005, 2006; *Khlopenkov and Trishchenko*, 2008]. For our purposes, a single clear-sky composite was created per year by merging the highest-quality pixels from multiple MODIS scenes during the period from July to September. This was done for each year between 2000 and 2008. The resulting composites represent minimum snow and ice (i.e., PSI) conditions for the ACA, an example of which for 2003 is shown in Figure 1. Nine regions of interest (ROI) were defined for the analysis of PSI (delineated in white in Figure 1), all of them featuring complex topography and areas permanently covered by snow and ice. Greenland as a large ice sheet was excluded from the analysis.

[8] Characteristic spectral surface properties of frozen water enable the discrimination of PSI from other land cover

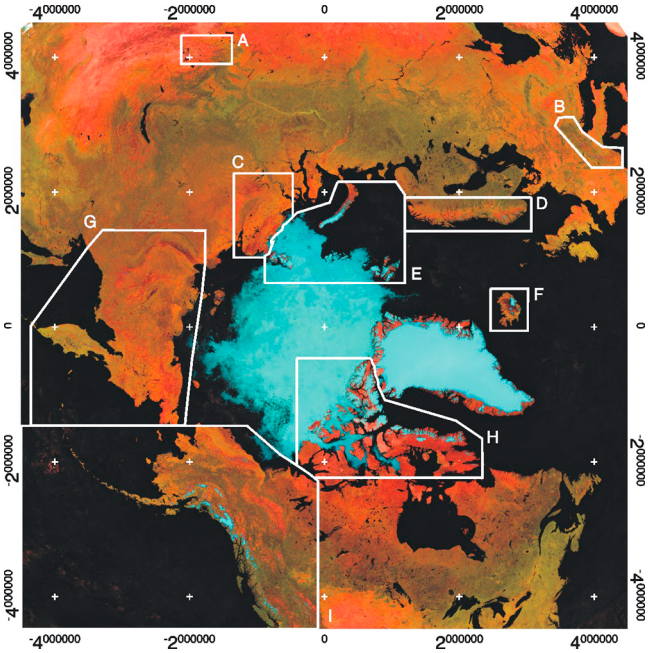

Figure 1. Arctic circumpolar clear−sky mosaic for July–September 2003 in Lambert Azimuthal Equal Area projection. Selected regions of interest are delineated in white and labeled according to Table 1. Perennial land (and sea) ice extent appears in bluish colors. Red shows band B6 (1.628–1.652 μm), green shows band B2 (0.841–0.876 μm), and blue shows band B1 (0.62–0.67 μm).

types [*Dozier and Painter*, 2004], if spectral data are available in the visible, near infrared, and shortwave infrared parts of the spectrum. Regarding the detection of snow and ice, the Normalized Difference Snow Index (NDSI) exploits the reflective properties of snow and ice covered surfaces. The NDSI is calculated by dividing the difference of reflectances observed in MODIS bands B4 and B6 by their sum and may be regarded as a measure of the abundance of snow and ice within the area covered by a pixel [*Salomonson and Appel*, 2004]. Hence, we generated MODIS PSI maps (PSI_{MODIS}) for each ROI and year similar to *Hall et al.* [2002], using a threshold of NDSI $\geq$ 0.4 and excluding pixels if either the B2 or B4 reflectance was <10%. It is important to note that debris-covered glacier surfaces are not recognized by this approach, because the spectral properties of supraglacial debris and the surrounding (snow- and ice-free) areas are similar [*Paul et al.*, 2004]. Supraglacial debris cover varies significantly between glaciers and geographic regions [*Konovalov*, 2000; *Paul et al.*, 2004; *Andreassen et al.*, 2008; *Molnia*, 2008]. We argue, however, that the areal extent of debris cover does not exhibit substantial interannual variability and will therefore not affect our results. In order to remove sea and lake ice prior to the analyses, a land-water mask was generated and applied based on the Global Self-consistent, Hierarchical, High-resolution Shoreline (GSHHS) database [*Wessel and Smith*, 1996].

2.2. Global Land Cover 2000 Data Set

[9] The Global Land Cover 2000 (GLC-2000) project [*Bartholomé and Belward*, 2005] (Global Land Cover 2000 database, 2004, available at http://bioval.jrc.ec.europa.eu/products/glc2000/products.php) led by the Joint Research Centre (JRC) of the European Commission (EC) aimed at generating a global land cover database in support of international programs such as the Millennium Ecosystems Assessment. The GLC-2000 land cover classification primarily made use of daily global mosaics of Satellite Pour l'Observation de la Terre (SPOT) VEGETATION 1 km satellite data acquired between November 1999 and December 2000. Other data sources were partially used to overcome limitations due to persistent cloud cover. Apart from regionally optimized land cover information the database also encompasses a single harmonized, yet thematically less detailed, global product [*Bartholomé and Belward*, 2005]. The global land cover legend includes 22 classes, following the Land Cover Classification System (LCCS) of the Food and Agriculture Organisation (FAO) [*Di Gregorio and Jansen*, 2000].

[10] In order to enable the areal comparison of PSI extent between GLC-2000 and MODIS circumpolar imagery, global GLC-2000 data were reprojected from original latitude/longitude to the LAEA projection (1 km spatial resolution). Land cover class 21 ("Snow and ice") was extracted to create PSI maps from GLC-2000 (PSI_{GLC}). Given the time period considered for the GLC-2000 classification scheme, PSI_{MODIS} was compared to PSI_{GLC} in 2000.

2.3. Globcover Land Cover Map

[11] The Globcover project launched in 2004 by the European Space Agency (ESA) had the objective to complement and update existing land cover classifications such as the GLC-2000 classification (section 2.2) with a new global land cover map for the year 2005 [*Arino et al.*, 2008] (Globcover land cover database, 2008, available at http://ionia1.esrin.esa.int/). The Globcover land cover map is based on 300 m spatial resolution data acquired between December 2004 and June 2006 by the Medium Resolution Imaging Spectrometer (MERIS) onboard Environmental Satellite (ENVISAT). The database includes a global product as well as eleven regional products as described by *Bicheron et al.* [2008]. Data gaps were filled using a set of reference land cover data sets. The legend of the global product includes 22 classes and is compatible with the LCCS mentioned in section 2.2.

[12] For consistency with the MODIS data, global Globcover data were reprojected from original latitude/longitude to the LAEA projection (300 m spatial resolution). PSI maps (PSI_{GC}) were obtained by extracting land cover class 220 ("Permanent snow and ice"). The decision on which year to select for the comparison of PSI_{MODIS} and PSI_{GC} is not straightforward, since the time period considered for the Globcover classification includes summer months both in 2005 (entire summer and fall) and 2006 (until June). We argue, however, that minimum snow and ice conditions are not achieved until June in most mountain regions and therefore compared PSI_{GC} to PSI_{MODIS} in 2005.

3. Results and Discussion

3.1. Interannual Variations of Perennial Snow and Ice Extent

[13] Results of the PSI_{MODIS} extent analysis for the period from 2000 to 2008 are summarized in Table 1. Overall, we

Table 1. Results of the Perennial Snow and Ice Extent Analysis for All Nine Regions of Interest Between 2000 and 2008[a]

ROI	Mean (km^2)	CV (%)	PSI_{MIN} / PSI_{MAX} (km^2)
A. Altai	1.33×10^3	14	$1.02 \times 10^3/1.63 \times 10^3$
B. European Alps	2.60×10^3	25	$1.93 \times 10^3/4.16 \times 10^3$
C. Northern Siberia	1.30×10^3	81	$4.96 \times 10^2/3.72 \times 10^3$
D. Scandinavia	4.98×10^3	50	$2.84 \times 10^3/1.08 \times 10^4$
E. Russian Arctic and Svalbard	1.04×10^5	5	$9.67 \times 10^4/1.11 \times 10^5$
F. Iceland	1.10×10^4	7	$1.05 \times 10^4/1.30 \times 10^4$
G. Eastern Siberia	3.96×10^3	67	$1.77 \times 10^3/9.94 \times 10^3$
H. Canadian Arctic	2.01×10^5	10	$1.71 \times 10^5/2.36 \times 10^5$
I. Western North America	1.32×10^5	13	$1.11 \times 10^5/1.67 \times 10^5$
All ROIs	4.94×10^5	22	$4.23 \times 10^5/5.26 \times 10^5$

[a]The ROIs are labeled according to Figure 1. CV is coefficient of variation, defined as the standard deviation divided by the mean multiplied by 100.

found PSI extent to exhibit strong interannual variations depending on the ROI. The coefficients of variation (CV), defined as the ratio of the standard deviation to the mean value over the 2000–2008 period, ranged from 5% in the Russian Arctic and Svalbard to 81% in Northern Siberia. In general, the observed interannual variability was particularly large in ROIs characterized by relatively small PSI extent (Table 1, A–D and G). Over all ROIs, PSI_{MODIS} extent varied with a CV of 22%. In order to illustrate interannual PSI_{MODIS} variations in more detail, selected geographic subsets within the European Alps and Northern Siberia ROIs are displayed in Figures 2 and 3, respectively. The PSI masks derived as described in section 2.1 are also shown.

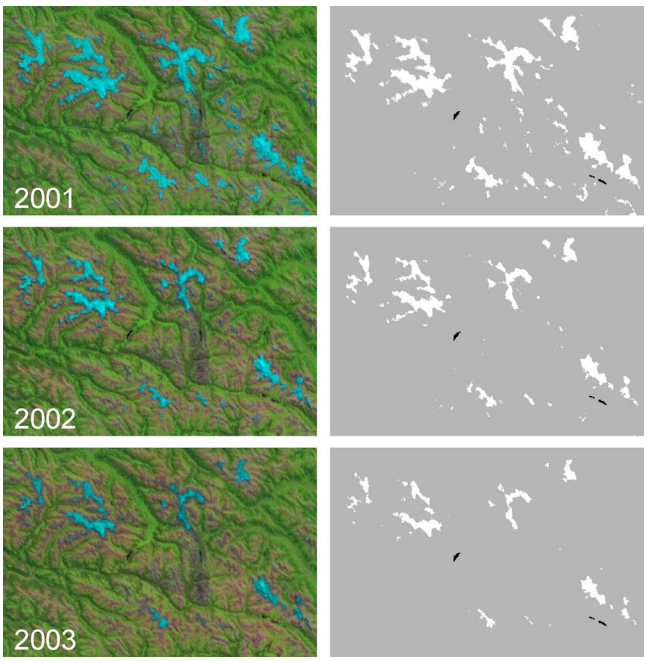

Figure 2. A subset of the European Alps ROI, located in the Eastern Swiss/Western Austrian Alps, as seen in (left) MODIS circumpolar composites between 2001 and 2003; (right) the corresponding PSI mask (delineated in white). The selected years represent (top) extensive, (middle) about average, and (bottom) below average PSI conditions. The subset covers an area of 150 km × 100 km. Water surfaces are marked in black in Figure 2 (right).

Figures 2 and 3 highlight the large interannual variability, which may be observed in certain ROIs, and demonstrate the range of spatial details provided by the circumpolar MODIS composites for the detection of PSI in mountain areas. Note the sea ice along the adjacent coast in Figure 3 in 2004, which comes along with extensive PSI extent in the displayed subset.

[14] Given that the extent of perennial mountain ice generally only varies slowly in time [*Oerlemans*, 2001], its variability is unlikely to be captured by MODIS imagery at 250 m spatial resolution except in cases of pronounced year-to-year ice retreat or advance. This is why, for detailed mapping of glacier extent, the GCOS has defined a spatial resolution of 30 m or finer. Hence, the variations in PSI_{MODIS} as outlined above can mainly be attributed to variations in perennial snow cover, even though variations in perennial snow cover on top of the glacier ice are not detected due to

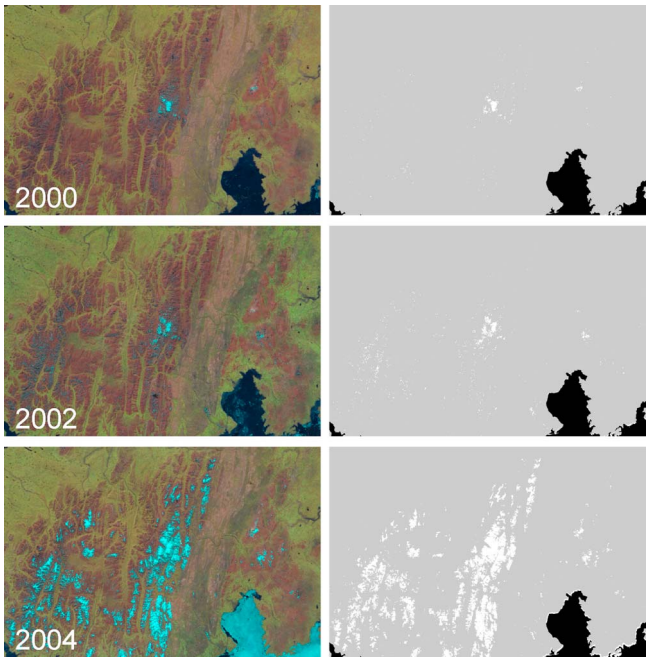

Figure 3. Similar to Figure 2, but for a subset of the same areal extent within the Northern Siberia ROI (northern Taimyr Peninsula) in 2000, 2002, and 2004. Note the sea ice cover that is accounted for by the land-water mask.

Table 2. Linear Correlation Coefficients (r_{Tpos}) Between Standardized Anomalies of PSI_{MODIS} and Positive Degree-Days (Threshold 0°C) During Selected Summer Months (2000–2008)[a]

ROI	May	Jun	Jul	Aug	Sep	May–Sep	Jun–Jul	Jun–Aug	Jun–Sep	Jul–Sep
A	0.09	0.17	−0.72*	−0.52	−0.56	−0.52	−0.62	−0.63	−0.72*	−0.77*
B	0.18	−0.58	−0.33	0.18	−0.55	−0.37	−0.61	−0.30	−0.50	−0.36
C	−0.54	−0.22	−0.04	−0.79*	0.12	−0.60	−0.19	−0.60	−0.59	−0.78*
D	−0.04	−0.56	−0.48	−0.51	−0.37	−0.61	−0.71*	−0.68*	−0.69*	−0.62
E	−0.09	−0.57	−0.02	0.64	−0.26	−0.01	−0.37	0.13	−0.02	0.20
F	0.19	−0.77*	−0.60	−0.42	0.08	−0.37	−0.90**	−0.75*	−0.54	−0.36
G	−0.25	−0.25	0.19	−0.78*	−0.57	−0.75*	−0.02	−0.58	−0.81**	−0.78*
H	0.03	−0.39	−0.17	−0.81**	0.27	−0.53	−0.25	−0.54	−0.52	−0.50
I	−0.75*	−0.60	−0.49	−0.75*	−0.03	−0.90**	−0.56	−0.70*	−0.77*	−0.73*

[a]Statistically significant values of r_{Tpos} are denoted with one ($p < 0.05$) or two ($p < 0.01$) asterisks. Results are provided for all nine ROIs according to Table 1 and Figure 1.

the limitations of the selected approach to distinguish between snow and ice. Observed large variability of PSI is in line with earlier studies that pointed at interannual variations of PSI in mountain regions [*Wang and Xie*, 2009] or, on larger scales, of Northern Hemisphere snow cover in summer [*Robinson et al.*, 1993]. Variations in snow cover have previously been shown to be negatively related to air temperature variations [*Robinson and Dewey*, 1990; *Brown*, 2000], owing to the snow-albedo feedback, which itself is assumed to be enhanced in mountain regions [*Giorgi et al.*, 1997; *Fyfe and Flato*, 1999]. However, the large scale atmospheric circulation conditions for a particular season, such as the predominant transport of warm/cold and wet/dry air masses, may constitute a very important factor responsible for the observed dependence.

[15] In order to place our findings in this context, we investigated the degree to which observed variations in PSI_{MODIS} can be explained by variations in air temperature during the summer season. For that purpose, we calculated positive degree-days (T_{pos}; threshold 0°C) based on 2 m temperature analysis data at 00, 06, 12, and 18 GMT between May and September. The temperature data at 0.5° spatial resolution were obtained from the European Centre for Medium-Range Weather Forecasts (ECMWF; www.ecmwf.int). All grid points representing land surfaces were averaged to obtain one single T_{pos} value per ROI and year. Linear correlation coefficients (r_{Tpos}) between standardized anomalies of PSI_{MODIS} and T_{pos} and their statistical significance are provided in Table 2. Standardized anomalies of PSI_{MODIS} and T_{pos} were computed by subtracting the mean for the period 2000–2008 from the raw data and dividing by the corresponding standard deviation for the same period. In agreement with the studies as mentioned above, we found strong and statistically significant negative correlations between standardized anomalies of T_{pos} and PSI_{MODIS} for most ROIs. In some cases, closest agreements were obtained for positive degree-days in single months, e.g., for the Canadian Arctic in August. Other ROIs exhibited strongest correlations for positive degree-days over more than one month, e.g., western North America for the period from May to September. As an additional illustration, standardized anomalies of PSI_{MODIS} and T_{pos} are shown in Figure 4. In agreement with the negative values of r_{Tpos} time series of PSI_{MODIS} and T_{pos} exhibit opposite behavior in time for most ROIs. Even though no statistically significant values of r_{Tpos} were obtained for the European Alps, Figure 4b highlights an interesting point: exceptionally warm and dry conditions during the summer heat wave in Central Europe from May to the end of August 2003 [*Black et al.*, 2004] are reflected in a strong positive T_{pos} anomaly and come along with a marked decrease in PSI_{MODIS} in the European Alps (see also Figure 2).

[16] In the northernmost ROIs (Figures 4c, 4e, 4g, and 4h) sea ice cover potentially is an important factor influencing PSI extent (see also Figure 3). Sea ice cover significantly affects climate in polar regions through the ice-albedo feedback and the insulation of the ocean [*Lemke et al.*, 2007] and may therefore influence the duration of the melt season in polar land areas [*Sharp and Wang*, 2009]. However, we found the PSI_{MODIS}-T_{pos} relationship to be statistically insignificant for the Russian Arctic and Svalbard, which is in contradiction to the findings of *Sharp and Wang* [2009], who describe a correlation between melt durations on glaciers and ice caps in Svalbard, Novaya Zemlya, and Severnaya Zemlya (three archipelagos within the ROI in Figure 4e) and June temperature at 850 hPa.

[17] Even though strongly negative values of r_{Tpos} point to a close connection between summer temperature and PSI extent in most ROIs, not all of the variance of PSI_{MODIS} could be explained by T_{pos}. Two possible explanations are that first, the mass balance of perennial snow patches was shown to be correlated not only to air temperature in summer, but also to precipitation in winter [*Higuchi*, 1975], which may lead to discrepancies in certain ROIs. Second, since we average all grid points of a T_{pos} field over land to obtain one single value per ROI and year, standardized anomalies of T_{pos} may not be representative of some temperature patterns unique to the mountain areas within the ROIs.

[18] Given the dependence of PSI on the meteorological conditions governing the accumulation (mainly in winter and spring) and the ablation processes of snow (primarily during the summer season), we would expect PSI_{MODIS} to be related to the net mass balance (b_n [m water equivalent]) of mountain glaciers. A net glacier mass balance for a specific year and glacier is also governed by the annual meteorological conditions and is an important and actively studied parameter in mountain regions [*Zemp et al.*, 2009]. It is equal to the sum of the observed winter and summer balances, which both represent a direct and immediate response of the glaciers' thickness and volume to annual atmospheric conditions [*Haeberli and Hoelzle*, 1995]. To test this relationship we compiled and averaged independently derived net mass balances of ten glaciers in the European Alps and

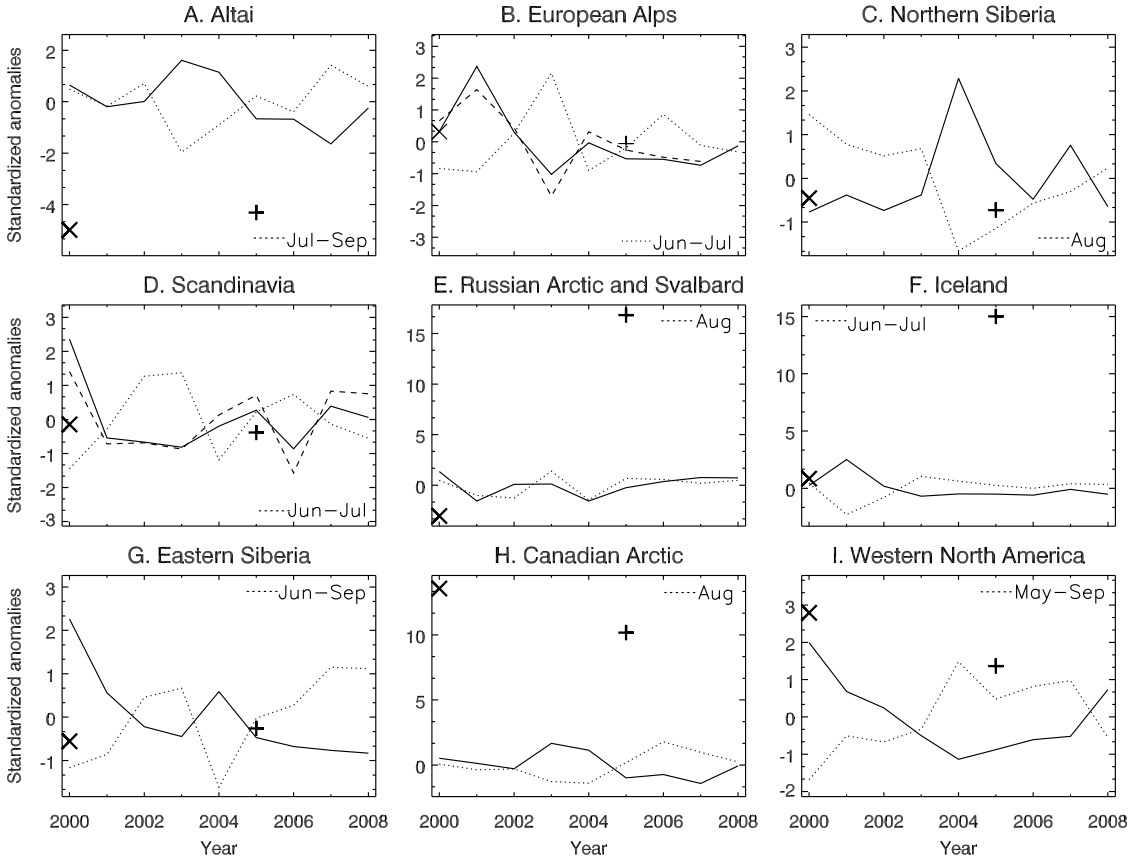

Figure 4. Standardized anomalies of perennial snow and ice (PSI) extent (solid line) and seasonally positive degree-days (T_{pos}, threshold 0°C; dotted line) for all nine regions of interest: (a) Altai, (b) European Alps, (c) Northern Siberia, (d) Scandinavia, (e) Russian Arctic and Svalbard, (f) Iceland, (g) Eastern Siberia, (h) Canadian Arctic, and (i) western North America. Standardized anomalies of T_{pos} are displayed for the periods where maximum absolute values of the linear correlation coefficient (r_{Tpos}) were obtained. Corresponding r_{Tpos} are provided in Table 2. Standardized anomalies of averaged net glacier mass balances (dashed line) are provided for the European Alps (ten glaciers, 2000–2007) and Scandinavia (six glaciers, 2000–2008). PSI_{GLC} in 2000 ("X" sign) and PSI_{GC} extent in 2005 (plus sign) are also displayed (standardized relative to PSI_{MODIS}).

six glaciers in Scandinavia to generate standardized anomalies of mean b_n. These two ROIs were chosen since b_n data were available for glaciers well distributed within the respective ROIs and for the entire time period (Scandinavia) and until 2007 (European Alps). Glacier mass balance data for the glaciers listed in Table 3 were obtained from the World Glacier Monitoring Service (WGMS; www.wgms.ch) and the Norwegian Water Resources and Energy Directorate (NVE) [*Andreassen et al.*, 2009].

[19] Standardized anomalies of b_n are provided in Figures 4b and 4d. A close, statistically significant ($p < 0.01$), positive relationship between standardized anomalies of PSI_{MODIS} and b_n was obtained, with linear correlation coefficients (r_{b_n}) of $r_{b_n} = 0.91$ (European Alps) and $r_{b_n} = 0.85$ (Scandinavia). A possible explanation for this close relationship is that in a given area, the average elevation of the snow line observed at the end of the summer season is inversely correlated with the extent of PSI_{MODIS} and directly related to the snow line observed on the glacier. The glacier's snow line, on its part, defines the elevation above which the glacier ice is covered by perennial snow and névé and can be regarded as a rough approximation of the glacier's equilibrium line in a given year [*Paterson*, 1994]. As such, it is directly correlated to the annual b_n. Results therefore suggest that PSI_{MODIS}, as a parameter reflecting the areal extent of snow (and ice) cover, may be regarded as an informative indicator of the (volumetric) parameter b_n in the mountain areas of Scandinavia and the European Alps. These results are of particular interest with regard to the requirement for information on glacier mass balances over larger spatial scales [*Lemke et al.*, 2007] and could serve as a useful tool for the integration of local measurements made at a few generally small glaciers over larger regions.

[20] From a hydrological point of view, the close negative PSI_{MODIS}-T_{pos} relationship is interesting with regard to future climate variations. A potential decrease in PSI extent (and, hence, in water availability) due to temperature increase could lead to increased competition for water resources in some mountain regions and surrounding lowlands [*Barnett et al.*, 2005]. From a climatological point of view, accurate knowledge of PSI extent is important in consideration of the strong influence of snow and ice on the

Table 3. Glaciers in the European Alps and Scandinavia ROIs Considered for the Calculation of the Mean Net Glacier Mass Balances[a]

Glacier[b]	Latitude/Longitude (°N/°E)	Area (km^2)
European Alps		
Sarennes (F)	45.14/6.14	0.5
Saint Sorlin (F)	45.17/6.15	3.0
Gries (CH)	46.44/8.34	5.3
Basòdino (CH)	46.42/8.48	2.2
Silvretta (CH)	46.85/10.08	2.9
Jamtalferner (A)	46.87/10.17	3.5
Hintereisferner (A)	46.80/10.77	7.4
Vernagtferner (A)	46.88/10.82	8.4
Stubacher Sonnblickkees (A)	47.13/12.60	1.4
Caresèr (I)	46.45/10.70	2.8
Scandinavia		
Rembesdalsskåka (N)	60.53/7.37	17.1[c]
Ålfotbreen (N)	61.75/5.65	4.5
Nigardsbreen (N)	61.72/7.13	47.8
Storbreen (N)	61.57/8.13	5.4
Engabreen (N)	66.65/13.85	38.7[c]
Langfjordjøkelen (N)	70.12/21.77	3.2[c]

[a]Glacier areal extent from *Haeberli et al.* [2008].
[b]Country abbreviations given in parentheses: F, France; CH, Switzerland; A, Austria; I, Italy; N, Norway.
[c]From *Andreassen et al.* [2009].

surface energy budget. The validation of PSI extent in LSCs used to derive land surface parameter data sets for climate models is therefore an important task. This will be discussed in the section 3.2.

3.2. Circumpolar MODIS Imagery Versus Other Land Surface Classifications

[21] The absolute and relative differences between PSI_{MODIS} and PSI from the two LSCs (PSI_{GLC} and PSI_{GC}) are provided in Table 4. In addition, Figure 4 illustrates PSI extent in both LSCs (standardized relative to PSI_{MODIS}). In certain cases, namely for the European Alps, Iceland, and western North America, there is a relatively good agreement between PSI_{MODIS} and PSI_{GLC} with relative discrepancies <10%. However, PSI_{GLC} and PSI_{GC}, in particular, differ significantly from PSI_{MODIS} in the majority of the cases. For some ROIs such as the Canadian Arctic (both LSCs) or Iceland (Globcover), we observed large differences (>100%). Over all ROIs, GLC-2000 (Globcover) overestimates PSI extent by 47% (86%). To illustrate the discrepancies between the data sets, Figures 5 and 6 display subsets of the circumpolar composites. Except for the Canadian Arctic ROI (Figures 5a and 6a), small subsets were selected to show PSI extent in more detail. Consistent with the statistics provided in Table 4, the overestimation of PSI extent in both LSCs is clearly apparent in the Canadian Arctic ROI. Figure 5b demonstrates for a small subset in the European Alps that GLC-2000 accurately classifies PSI in 2000 for this area. In contrast, PSI is underestimated by GLC-2000 in the Altai mountain range Figure 5c. Similarly, Figure 6b shows an example in the European Alps where the discrepancies between PSI_{MODIS} and PSI_{GC} were small. However, in Northern Siberia PSI extent was found to be clearly underestimated in the Globcover product (Figure 6c).

[22] The magnitude of the obtained differences in PSI extent for some ROIs was somewhat surprising. As for the Globcover classification, sparse data collection of the MERIS instrument due to a smaller swath width compared to MODIS (1150 km versus 2330 km) may result in discrepancies because this reduces the chance of a geographic location being observed under clear-sky and snow-free conditions. This particularly applies to mountain and polar regions, as these are often characterized by persistent cloud cover and fog. As a consequence, snow and ice are likely to prevent observations of the underlying land surface, resulting in large deviations relative to PSI_{MODIS}. Apparently, the number of valid observations obtained after 19 months of MERIS acquisitions is limited in most of the ROIs selected here [*Bicheron et al.*, 2008, Figure 9]. Additional errors could be introduced to the Globcover product where a reference data set was used to fill gaps due to missing data, and users are asked to consult the information provided in the corresponding quality flag [*Bicheron et al.*, 2008]. Here the use of a reference data set is a potential source of error for two reasons: first, potential errors in the reference data sets could propagate into the Globcover database. Second, reference data sets do not necessarily originate from the same observation period as the Globcover product (e.g., the GLC-2000 classification) and, hence, do not accurately reproduce PSI extent in cases of strong interannual PSI variability as described above. This also points at a general problem of classifying permanently snow and ice covered surfaces. Due to the strong interannual variability of PSI extent observed in some ROIs, the informative value of this land cover class in LSCs is somewhat limited.

Table 4. Absolute and Relative Differences of PSI Extent as Extracted From the Global Land Cover (GLC-2000) as Well as Globcover Land Surface Classifications With Respect to PSI_{MODIS}[a]

		GLC-2000			Globcover 2005	
ROI	PSI_{MODIS} 2000 (km^2)	Absolute (km^2)	Relative (%)	PSI_{MODIS} 2005 (km^2)	Absolute (km^2)	Relative (%)
A	1.45×10^3	-1.06×10^3	−73	1.21×10^3	-6.85×10^2	−57
B	2.82×10^3	−5	0	2.25×10^3	3.15×10^2	14
C	4.96×10^2	3.31×10^2	67	1.66×10^3	-1.12×10^3	−68
D	1.08×10^4	-6.22×10^3	−57	5.66×10^3	-1.63×10^3	−29
E	1.11×10^5	-2.12×10^4	−19	1.03×10^5	8.25×10^4	80
F	1.12×10^4	4.77×10^2	4	1.06×10^4	1.22×10^4	115
G	9.94×10^3	-7.45×10^3	−75	2.72×10^3	5.55×10^2	20
H	2.12×10^5	2.71×10^5	128	1.80×10^5	2.32×10^5	129
I	1.67×10^5	1.42×10^4	8	1.16×10^5	3.98×10^4	34
All	5.26×10^5	2.50×10^5	47	4.23×10^5	3.64×10^5	86

[a]Differences indicated for GLC-2000 (Globcover) refer to PSI_{MODIS} in 2000 (2005). Positive (negative) values denote cases, where the land cover products overestimate (underestimate) PSI extent. Results are provided for all nine ROIs according to Table 1 and Figure 1.

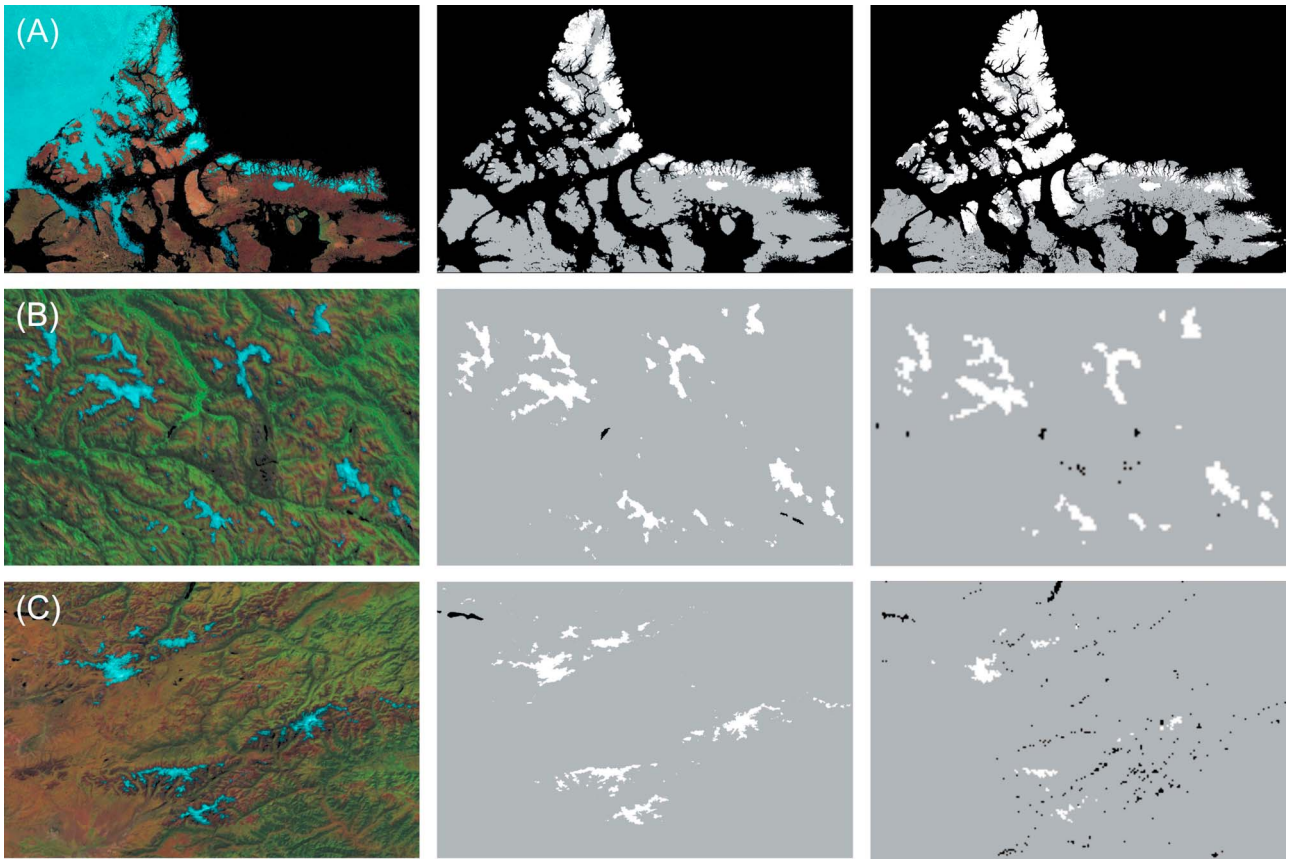

Figure 5. (left) MODIS circumpolar false color imagery in 2000, (middle) corresponding PSI_{MODIS}, and (right) PSI_{GLC}. Three areas are displayed: (a) the northern Canada ROI (2750 × 1775 km^2), (b) a subset of the European Alps ROI(150 × 100 km^2), and (c) a subset of the Altai mountain range within the Altai ROI (255 × 166 km^2). While there is a good agreement between PSI_{MODIS} and PSI_{GLC} in the European Alps, the extent of PSI is clearly overestimated (underestimated) in the Canadian Arctic ROI (Altai subset) by the GLC-2000 classification (see Table 4). Color code for the PSI maps: white, PSI; black, water surfaces; grey, snow- and ice-free land surfaces.

[23] Regarding the GLC-2000 classification, differences in the spatial resolution of the classification are one possible reason for the observed discrepancies. For example, small snow patches may not be included at 1 km spatial resolution. However, this can certainly not explain the large deviations we observed in some ROIs. In the Canadian Arctic, the ROI with the most extensive PSI extent, areas north of approximately 72°N revealed the largest discrepancies. For GLC 2000, one can speculate that this can be related to mixing VEGETATION data with data from other sensors such as MODIS between 75°N–80°N and the Advanced Very High-Resolution Radiometer (AVHRR; 80°N–90°N) to produce results for polar regions(Global Land Cover 2000 database, update information for version 1, 2004, available at http://bioval.jrc.ec.europa.eu/products/glc2000/products/Update_version1.pdf).

[24] With regard to LSCs being used to derive land surface parameter data sets, such as background surface albedo, for use in climate and land surface process models, the accurate delineation of PSI in land cover products is important, since the output of such models has been shown to be sensitive to land surface boundary conditions [*Garratt*, 1993]. While the impact of PSI misclassification on the assessment of land surface–atmosphere fluxes is assumed to be limited to local scales for ROIs exhibiting small PSI extent (e.g., the Altai mountain range or Northern Siberia), it is likely to be more relevant for simulations at larger scales for ROIs characterized by large areas of PSI (e.g., Canadian Arctic or western North America). However, the quantification of this impact remains to be addressed in future studies.

4. Concluding Remarks

[25] Perennial snow and ice extent represents minimum snow and ice conditions in mountain regions at the end of the summer season and reflects the balance of accumulation and melting processes during the previous seasons. We made use of a novel MODIS data set developed by the Canada Centre for Remote Sensing at 250 m spatial resolution and covering the Arctic circumpolar area to quantify interannual variations in PSI extent between 2000 and 2008. To our knowledge this is the first-ever attempt to study the annual PSI variations using a consistent satellite data set at 250 m spatial resolution. Nine ROIs were selected, all of which cover mountain areas to a certain extent. Depending

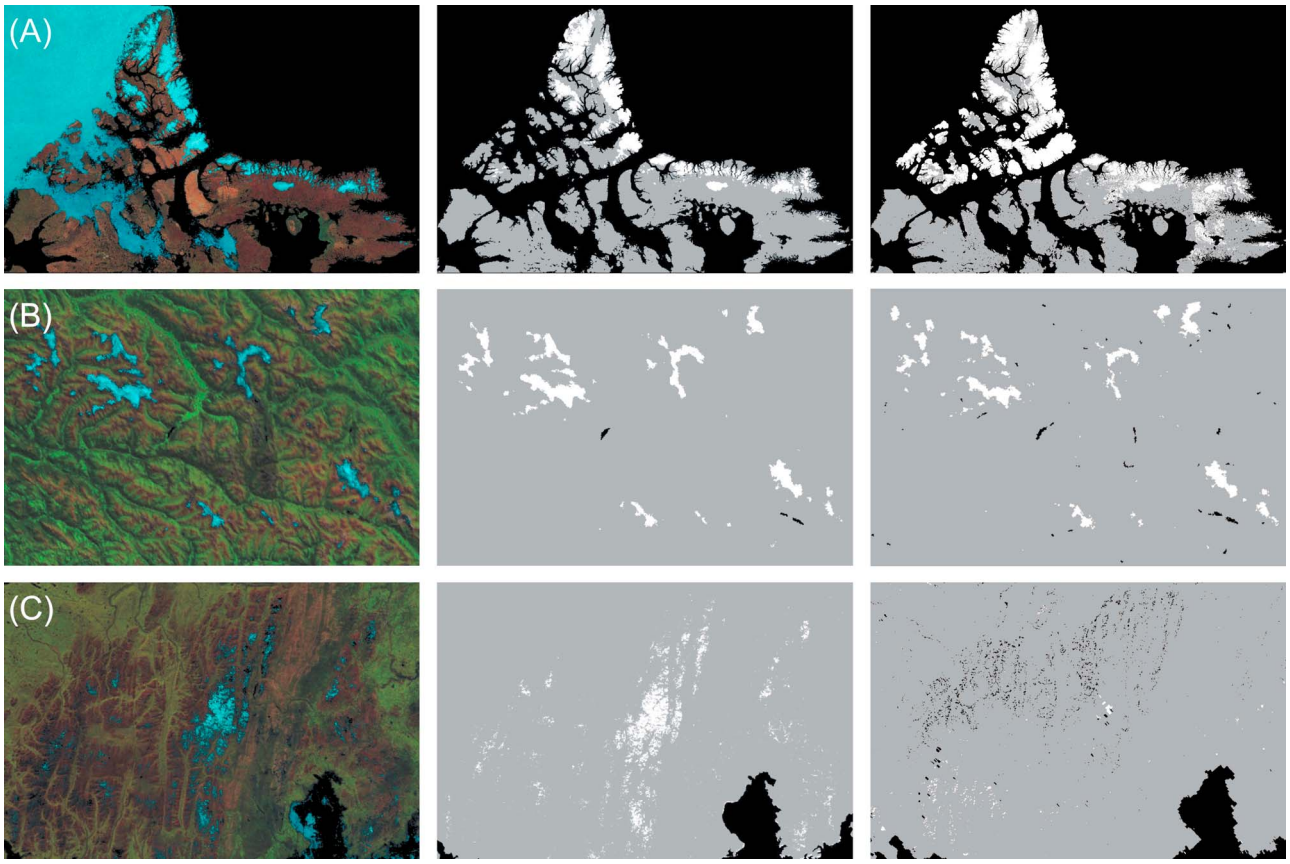

Figure 6. (left) MODIS circumpolar false color imagery in 2005, (middle) corresponding PSI_{MODIS}, and (right) PSI_{GC}. Three areas are displayed: (a) the northern Canada ROI (2750 km × 1775 km), (b) a subset of the European Alps ROI (150 km × 100 km), and (c) a subset of the Northern Siberia ROI (150 km × 100 km). In contrast to a relatively good agreement in the European Alps, the extent of PSI is clearly overestimated in PSI_{GC} for the Canadian Arctic ROI but underestimated in Northern Siberia (see Table 4). Color code for the PSI maps: white, PSI; black, water surfaces; grey, snow- and ice-free land surfaces.

on the ROI, large interannual variability of PSI was detected. These data show a good correlation with positive degree-days during the summer season, likely reflecting the strong snow-albedo feedback in mountain regions. In addition, independent time series of averaged net glacier mass balances collected over the European Alps and Scandinavia showed a very close agreement with PSI extent, which suggests that PSI variations could serve as an indicator of net glacier mass balances. This is of particular interest with regard to the need for integrated information on glacier mass balances on broad spatial scales. Overall, the understanding of such PSI variations is critical with respect to the importance of snow and ice for the hydrological cycle in mountain regions and surrounding lowlands. Changes in the spatial extent of PSI reflect changes in the amount of water stored in mountain regions, and hence, changes in water availability at the end of the summer season. In light of the close negative relationship between PSI extent and the climatic conditions, climate warming projected for the future may result in increased competition for water resources in some regions.

[26] Finally, the circumpolar MODIS imagery was employed to validate PSI extent in two satellite-based land surface classifications, GLC-2000 and Globcover. Such analysis may be useful to evaluate the degree of uncertainty in using these data sets as a basis for land surface parameterizations in climate and land surface process models. PSI extent was found to be significantly different in both land surface classifications, which could be a potential source of error in modeling applications. This is of particular interest for large ROIs exhibiting extensive PSI coverage, as a misclassification of PSI in these areas may affect model output at large spatial scales through the snow-albedo effect and impacts on the water-energy balance. However, this remains to be quantified in future studies.

[27] In summary, circumpolar MODIS imagery has provided interesting and novel insight into PSI variations in several mountain ranges at high spatial resolution. Given the importance of snow and ice for many land surface and hydrological processes, the results presented here will enhance our understanding of future climate change impact in mountain regions.

[28] **Acknowledgments.** The work was conducted at the Canada Centre for Remote Sensing (CCRS), Earth Sciences Sector of the Department of Natural Resources Canada as part of the Project J35 of the Program on "Enhancing Resilience in a Changing Climate" and was supported through the Canadian IPY program. F. Fontana's work at the CCRS was funded by the Swiss National Science Foundation and the Oeschger Centre

for Climate Change Research, Switzerland. S. Nussbaumer has been funded by the Swiss National Science Foundation, grant 200021-116354. The MODIS data were acquired from the NASA Distributed Data Archive Center (DAAC; http://daac.gsfc.nasa.gov). ESA and the ESA Globcover Project led by MEDIAS France/POSTEL are acknowledged for provision of the Globcover data. GLC-2000 data were acquired from the Joint Research Centre of the European Commission.

References

Andreassen, L. M., F. Paul, A. Kääb, and J. E. Hausberg (2008), Landsat-derived glacier inventory for Jotunheimen, Norway, and deduced glacier changes since the 1930s, *Cryosphere*, *2*(2), 131–145.

Andreassen, L. M., H. Elvehøy, M. Jackson, B. Kjøllmoen, R. H. Giesen, and A. M. Tvede (2009), Glaciological investigations in Norway in 2008, *Rep. 2*, 80 pp., Norw. Water Resources and Energy Dir., Oslo.

Arino, O., P. Bicheron, F. Achard, J. Latham, R. Witt, and J. L. Weber (2008), GLOBCOVER—The most detailed portrait of Earth, *ESA Bull.*, *136*, 21–34.

Barnett, T. P., J. C. Adam, and D. P. Lettenmaier (2005), Potential impacts of a warming climate on water availability in snow-dominated regions, *Nature*, *438*(7066), 303–309.

Bartholomé, E., and A. S. Belward (2005), GLC2000: A new approach to global land cover mapping from Earth observation data, *Int. J. Remote Sens.*, *26*(9), 1959–1977.

Beniston, M. (2003), Climatic change in mountain regions: A review of possible impacts, *Clim. Change*, *59*(1), 5–31.

Bicheron, P., et al. (2008), GLOBCOVER: Products Description and Validation Report, report, MEDIAS Fr., Toulouse, France. (Available at http://ionia1.esrin.esa.int/index.asp)

Black, E., M. Blackburn, G. Harrison, B. Hoskins, and J. Methven (2004), Factors contributing to the summer 2003 European heatwave, *Weather*, *59*(8), 217–223.

Bonan, G. B., K. W. Oleson, M. Vertenstein, S. Levis, X. Zeng, Y. Dai, R. E. Dickinson, and Z.-L. Yang (2002), The land surface climatology of the community land model coupled to the NCAR community climate model, *J. Clim.*, *15*(22), 3123–3149.

Brown, R. D. (2000), Northern Hemisphere snow cover variability and change, 1915–1997, *J. Clim.*, *13*(13), 2339–2355.

Brown, R. D., and P. W. Mote (2009), The response of Northern Hemisphere snow cover to a changing climate, *J. Clim.*, *22*(8), 2124–2145.

Di Gregorio, A., and L. J. M. Jansen (2000), Land Cover Classification System (LCCS): Classification concepts and user manual, instruction manual, Nat. Resour. Manage. and Environ. Dep., Food and Agric. Org. of the U. N., Rome, Italy. (Available at http://www.fao.org/DOCREP/003/X0596E/X0596e00.htm)

Dozier, J., and T. H. Painter (2004), Multispectral and hyperspectral remote sensing of alpine snow properties, *Annu. Rev. Earth Planet Sci.*, *32*(1), 465–494.

Fyfe, J. C., and G. M. Flato (1999), Enhanced climate change and its detection over the Rocky Mountains, *J. Clim.*, *12*(1), 230–243.

Garratt, J. (1993), Sensitivity of climate simulations to land-surface and atmospheric boundary-layer treatments—A review, *J. Clim.*, *6*(3), 419–448.

Giorgi, F., J. W. Hurrell, M. R. Marinucci, and M. Beniston (1997), Elevation dependency of the surface climate change signal: A model study, *J. Clim.*, *10*(2), 288–296.

Giri, C., Z. Zhu, and B. Reed (2005), A comparative analysis of the Global Land Cover 2000 and MODIS land cover data sets, *Remote Sens. Environ.*, *94*(1), 123–132.

Global Climate Observing System (2006), Systematic observation requirements for satellite-based products for climate: Supplemental details to the satellite-based component of the "Implementation plan for the global observing system for climate in support of the UNFCCC," *Rep. GCOS-107*, Geneva, Switzerland.

Groisman, P., T. R. Karl, R. W. Knight, and G. L. Stenchikov (1994), Changes of snow cover, temperature, and radiative heat balance over the Northern Hemisphere, *J. Clim.*, *7*(11), 1633–1656.

Haeberli, W., and M. Hoelzle (1995), Application of inventory data for estimating characteristics of and regional climate-change effects on mountain glaciers: A pilot study with the European Alps, *Ann. Glaciol.*, *21*, 206–212.

Haeberli, W., M. Zemp, A. Kääb, F. Paul, and M. Hoelzle (Eds.) (2008), *Fluctuations of Glaciers 2000–2005*, vol. 9, 266 pp., World Glacier Monit. Serv., Zurich, Switzerland.

Hagemann, S. (2002), An improved land surface parameter dataset for global and regional climate models, Rep. 336, Max Planck Inst. for Meteorol., Hamburg, Germany.

Hall, D. K., G. A. Riggs, V. V. Salomonson, N. E. Di Girolamo, and K. J. Bayr (2002), MODIS snow-cover products, *Remote Sens. Environ.*, *83*(1–2), 181–194.

Hansen, M. C., and B. Reed (2000), A comparison of the IGBP DISCover and University of Maryland 1 km global land cover products, *Int. J. Remote Sens.*, *21*(6), 1365–1373.

Hauenstein, W. (2005), Hydropower and climate change—A reciprocal relation: Institutional energy issues in Switzerland, *Mt. Res. Dev.*, *25*(4), 321–325.

Higuchi, K. (1975), On the relation between mass balance of perennial snow patches and climatic variation in Central Japan, in *Snow and Ice Symposium: Proceedings of the Moscow Symposium, August 1971*, *IAHS Publ.*, *104*, 141–143.

Jansson, P., R. Hock, and T. Schneider (2003), The concept of glacier storage: A review, *J. Hydrol.*, *282*(1–4), 116–129.

Justice, C. O., et al. (1998), The Moderate Resolution Imaging Spectroradiometer (MODIS): Land remote sensing for global change research, *IEEE Trans. Geosci. Remote Sens.*, *36*(4), 1228–1249.

Kargel, J. S., et al. (2005), Multispectral imaging contributions to global land ice measurements from space, *Remote Sens. Environ.*, *99*(1–2), 187–219.

Khlopenkov, K. V., and A. P. Trishchenko (2008), Implementation and evaluation of concurrent gradient search method for reprojection of MODIS level 1B imagery, *IEEE Trans. Geosci. Remote Sens.*, *46*(7), 2016–2027.

Konovalov, V. (2000), Computations of melting under moraine as a part of regional modelling of glacier runoff, in *Debris-Covered Glaciers*, edited by M. Nakawo, C. F. Raymond, and A. Fountain, *IAHS Publ.*, *264*, 109–118.

Kotlarski, S. (2007), A subgrid glacier parameterisation for use in regional climate modelling, Ph.D. thesis, Max Planck Inst. for Meteorol., Hamburg, Germany.

Lemke, P., J. Ren, R. Alley, I. Allison, J. Carrasco, G. Flato, Y. Fujii, G. Kaser, P. Mote, R. Thomas, and T. Zhang (2007), Observations: Changes in snow, ice and frozen ground, in *Climate Change 2007: The Physical Science Basis: Contribution of Working Group I to the Fourth Assessment Report on the Intergovernmental Panel on Climate Change*, edited by S. Solomon et al., pp. 337–383, Cambridge Univ. Press, Cambridge, U. K.

Luo, Y., A. P. Trishchenko, and K. V. Khlopenkov (2008), Developing clear-sky, cloud and cloud shadow mask for producing clear-sky composites at 250-meter spatial resolution for the seven MODIS land bands over Canada and North America, *Remote Sens. Environ.*, *112*(12), 4167–4185.

Molnia, B. F. (2008), Glaciers of North America—Glaciers of Alaska, in *Satellite Image Atlas of Glaciers of the World*, edited by R. S. William and J. G. Ferrigno, 525 pp., *U.S. Geol. Surv. Prof. Pap.*, *1386-E*.

Nolin, A. W., and A. Frei (2001), Remote sensing of snow and characterization of snow albedo for climate simulations, in *Remote Sensing and Climate Modeling: Synergies and Limitations* edited by M. Beniston and M. M. Verstraete, pp. 159–180, Kluwer Acad., New York.

Oerlemans, J. (2001), *Glaciers and Climate Change*, 148 pp., A. A. Balkema, Rotterdam, Netherlands.

Paterson, W. S. B. (1994), *The Physics of Glaciers*, 3rd ed., 481 pp., Elsevier Sci., Oxford, U. K.

Paul, F., C. Huggel, and A. Kääb (2004), Combining satellite multispectral image data and a digital elevation model for mapping debris-covered glaciers, *Remote Sens. Environ.*, *89*(4), 510–518.

Paul, F., A. Kääb, and W. Haeberli (2007), Recent glacier changes in the Alps observed by satellite: Consequences for future monitoring strategies, *Global Planet. Change*, *56*(1–2), 111–122, doi:10.1016/j.gloplacha.2006.07.007.

Ramsay, B. H. (1998), The interactive multisensor snow and ice mapping system, *Hydrol. Processes*, *12*(10–11), 1537–1446.

Robinson, D. A., and K. F. Dewey (1990), Recent secular variations in the extent of Northern Hemisphere snow cover, *Geophys. Res. Lett.*, *17*, 1557–1560.

Robinson, D. A., K. F. Dewey, and R. R. Heim (1993), Global snow cover monitoring: An update, *Bull. Am. Meteorol. Soc.*, *74*(9), 1689–1696.

Romanov, P., G. Gutman, and I. Csiszar (2002), Satellite-derived snow cover maps for North America: Accuracy assessment, *Adv. Space Res.*, *30*(11), 2455–2460.

Salomonson, V. V., and I. Appel (2004), Estimating fractional snow cover from MODIS using the normalized difference snow index, *Remote Sens. Environ.*, *89*(3), 351–360.

Salomonson, V. V., W. L. Barnes, P. W. Maymon, H. E. Montgomery, and H. Ostrow (1989), MODIS: Advanced facility instrument for studies of the Earth as a system, *IEEE Trans. Geosci. Remote Sens.*, *27*(2), 145–153.

Sellers, P. J., S. O. Los, C. J. Tucker, C. O. Justice, D. A. Dazlich, G. J. Collatz, and D. A. Randall (1996), A revised land surface parametrization (SiB2) for atmospheric GCMs. Part II: The generation of global fields of terrestrial biophysical parameters from satellite data, *J. Clim.*, *9*(4), 706–737.

Sharp, M., and L. Wang (2009), A five-year record of summer melt on Eurasian Arctic ice caps, *J. Clim.*, *22*(1), 133–145.

Sirguey, P., R. Mathieu, and Y. Arnaud (2009), Subpixel monitoring of the seasonal snow cover with MODIS at 250 m spatial resolution in the Southern Alps of New Zealand: Methodology and accuracy assessment, *Remote Sens. Environ.*, *113*(1), 160–181.

Trishchenko, A. P., Y. Luo, and K. V. Khlopenkov (2006), A method for downscaling MODIS land channels to 250 m spatial resolution using adaptive regression and normalization, *Proc. SPIE Int. Soc. Opt. Eng.*, *6366*, 636607, doi:10.1117/12.689157.

Trishchenko, A. P., Y. Luo, K. V. Khlopenkov, W. M. Park, and S. Wang (2009), Arctic circumpolar mosaic at 250 m spatial resolution for IPY by fusion of MODIS/TERRA land bands B1–B7, *Int. J. Remote. Sens.*, *30*(6), 1635–1641.

United Nations Environment Programme (2007), Global outlook for snow and ice, report, GRID-Arendal, Arendal, Norway.

Vavrus, S. (2007), The role of terrestrial snow cover in the climate system, *Clim. Dyn.*, *29*(1), 73–88.

Wang, X., and H. Xie (2009), New methods for studying the spatiotemporal variation of snow cover based on combination products of MODIS Terra and Aqua, *J. Hydrol.*, *371*(1–4), 192–200.

Wessel, P., and W. H. F. Smith (1996), A global, self-consistent, hierarchical, high-resolution shoreline database, *J. Geophys. Res.*, *101*(B4), 8741–8743.

Wolfe, R. E., M. Nishihama, A. J. Fleig, J. A. Kuyper, D. P. Roy, J. C. Storey, and F. S. Patt (2002), Achieving sub-pixel geolocation accuracy in support of MODIS land science, *Remote Sens. Environ.*, *83*(1–2), 31–49.

Xiong, X., N. Che, and W. Barnes (2005), Terra MODIS on-orbit spatial characterization and performance, *IEEE Trans. Geosci. Remote Sens.*, *43*(2), 355–365.

Xiong, X., N. Che, W. Barnes, Y. Xie, L. Wang, and J. Qu (2006), Status of Aqua MODIS spatial characterization and performance, in *Proc. SPIE Int. Soc. Opt. Eng.*, *6361*, 63610T, doi:10.1117/12.687162.

Zemp, M., M. Hoelzle, and W. Haeberli (2009), Six decades of glacier mass-balance observations: A review of the worldwide monitoring network, *Ann. Glaciol.*, *70*, 101–111.

F. M. A. Fontana, S. U. Nussbaumer, and S. Wunderle, Institute of Geography and Oeschger Centre for Climate Change Research, University of Bern, Hallerstr. 12, CH-3012 Bern, Switzerland. (ffontana@interchange.ubc.ca)

K. V. Khlopenkov, Science Systems and Applications, Inc., 1 Enterprise Pkwy., Suite 200, Hampton, VA 23666, USA.

Y. Luo and A. P. Trishchenko, Environment Canada, 373 Sussex Dr., Ottawa, ON K1A 0H3, Canada.